On the structural, electronic and magnetic properties of $MnCr_2O_4$ spinel

1997 J. Phys.: Condens. Matter 9 10715

(http://iopscience.iop.org/0953-8984/9/48/014)

J. Phys.: Condens. Matter **9** (1997) 10715–10724. Printed in the UK PII: S0953-8984(97)85964-4

On the structural, electronic and magnetic properties of $MnCr_2O_4$ spinel

F Freyria Fava†, I Baraille‡, A Lichanot‡, C Larrieu‡ and R Dovesi†

† Department CIFM, University of Torino, via Giuria 5, I-10125 Torino, Italy

‡ Laboratoire de Chimie Structurale, UMR 5624, IFR rue Jules Ferry, 64000 Pau, France

Received 11 July 1997

Abstract. The structural, electronic and magnetic properties of $MnCr_2O_4$ spinel are investigated using the periodic *ab initio* Hartree–Fock program CRYSTAL. The geometry is fully optimized and the bulk modulus evaluated. The system is a large-gap insulator; the Mn–O bond is fully ionic, whereas in the Cr–O case there is a relatively large overlap between the Cr d and the O sp orbitals, and the resulting bond has some covalent character. The ferromagnetic solution (all spins in the same direction) and two ferrimagnetic solutions (one or two Mn atoms of the unit cell with spin down, the remaining transition metal atoms with spin up) have been considered; the latter are more stable than the former by 2.2 and 3.8 mHartree per unit cell, respectively. At zero pressure, the spinel is more stable than the mixture of simple oxides $MnO + \alpha$-Cr_2O_3 by about 17 kcal mol^{-1}, in excellent agreement with experiment.

1. Introduction

Powerful computational tools have been made available in the past few years for simulating *ab initio* ground-state properties of crystalline solids containing transition metal salts and/or having relatively large unit cells. The periodic Hartree–Fock scheme [1, 2], in particular, has been shown to be able to reproduce qualitatively and semi-quantitatively not only the structural and electronic properties of simple transition metal oxides such as MnO and NiO [3, 4], and of relatively complex structures such as Fe_2O_3 [5] and Cr_2O_3 [6], but also more delicate quantities such as the relative stability of different magnetic phases, in spite of the limitation related to the neglect of electron correlation. Recent improvements of the CRYSTAL95 computer code [7], both in terms of speed and of tools for addressing the required magnetic solution and for controlling the self-consistent-field process when many transition metal ions with open-shell structure are present in the unit cell, now permit the investigation of relatively complicated structures with more than one type of transition metal atom. The spinels AB_2O_4 [8] represent one of the most important and interesting families of crystalline compounds, with applications in many different areas. The present method has been applied in the past to the study of one of the simplest members of the family, namely $MgAl_2O_4$ [9]. The structural and elastic properties of this compound have been correctly reproduced, as well as its relative stability with respect to the simple oxides MgO and α-Al_2O_3. In the present paper, we investigate for the first time the structural, electronic and magnetic properties of a spinel with two different transition metal atoms, namely $MnCr_2O_4$. The structure of $MnCr_2O_4$, which contains two formula units per cell (14 atoms), has been optimized and the bulk modulus evaluated; the electronic properties will be discussed in terms of Mulliken population analysis data, band structures, densities

0953-8984/97/4810715+10$19.50

of states, and charge- and spin-density maps. The stability of the spinel with respect to MnO and α-Cr_2O_3 is calculated. As regards the magnetic properties, three structures have been considered which do not require large unit cells or a substantial symmetry reduction: the ferromagnetic system (FEM), in which all spins of the uncoupled electrons are up, and two ferrimagnetic solutions, with spins down for one (FIM_1) or two (FIM_2) Mn atoms in the unit cell (all Cr atoms having spin up).

2. Computational details

For the present calculations, the CRYSTAL95 computer program [7] has been used, which contains an unrestricted Hartree–Fock (UHF) option for the treatment of spin-polarized systems. This feature is necessary for obtaining spin-polarized eigenfunctions of the Fock Hamiltonian, because of the presence of unpaired 3d electrons on Cr and Mn. We refer the reader to previous papers [1, 2] for a description of the periodic Hartree–Fock crystalline-orbitals LCAO self-consistent-field computational scheme as implemented in the CRYSTAL95 code [7]; the UHF formulation for periodic systems and applications to transition metal compounds can be found in references [6–10]. Tools have been implemented in CRYSTAL95 in order to direct the system towards the required spin solution. It is, however, to be remembered that only the total number of unpaired electrons in the unit cell is imposed *a priori*, whereas no constraint at all is imposed on the partition of the spin density between the transition metal atoms (four Cr and two Mn in the present case), and among the d orbitals of a given atom. The final spin configuration in the unit cell is then the result of a variational calculation, with the constraint of the number of $\alpha - \beta$ electrons being defined *a priori*. As regards the computational conditions, the numerical values of the tolerance parameters involved in the evaluation of the infinite bielectronic Coulomb and exchange series were identical to those adopted in recent studies [3–6], and were chosen to ensure high numerical accuracy. The shrinking factor, S, defining the reciprocal space net is 4, corresponding to eight reciprocal-space points in which the Fock matrix is diagonalized. When $S = 8$ is used, the energy difference with respect to the $S = 4$ case is smaller than 10^{-5} Hartree/cell. As regards the basis set, Bloch functions are constructed from local functions ('atomic orbitals'), which in turn are linear combinations ('contractions') of gaussian-type functions (GTFs), and each of these is a product of a gaussian and a real solid spherical harmonic. The all-electron basis set used for the present study is very similar to that used in previous studies on Cr_2O_3 (with a Cr and O basis set) [6] and MnO (with a Mn basis set) [3], and contains 13 atomic orbitals for O and 27 for each of Cr and Mn. The oxygen basis set can be denoted as an 8-411G contraction (the first shell is of s type and is a contraction of eight GTFs; then there are three sp shells). For Cr and Mn, an 8-6-411-(41 d)G contraction is used, with two d-type shells. The exponents of the most diffuse sp and d shells of the three atoms have been optimized by searching for the minimum crystalline total energy. The best values (α_{sp}(Mn) = 1.21 and 0.50; α_{sp}(O) = 0.49 and 0.20; α_{sp}(Cr) = 1.16 and 0.49; α_{d}(Cr) = 0.34; α_{d}(Mn) = 0.25) are very close to those optimized for Cr_2O_3 and MnO.

3. Results and discussion

3.1. Structure

$MnCr_2O_4$ has the 'normal' (as opposed to 'inverse') spinel structure (space group $Fd3m$), with two formula units in the unit cell (14 atoms). The Cr and Mn atoms are at $(\frac{1}{2}, \frac{1}{2}, \frac{1}{2})$

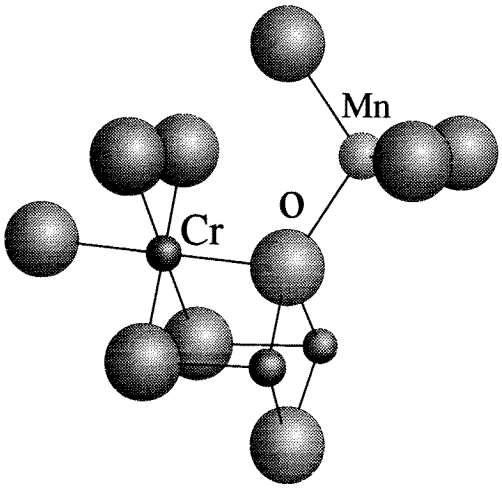

Figure 1. First-neighbour coordination for Mn, Cr and O atoms.

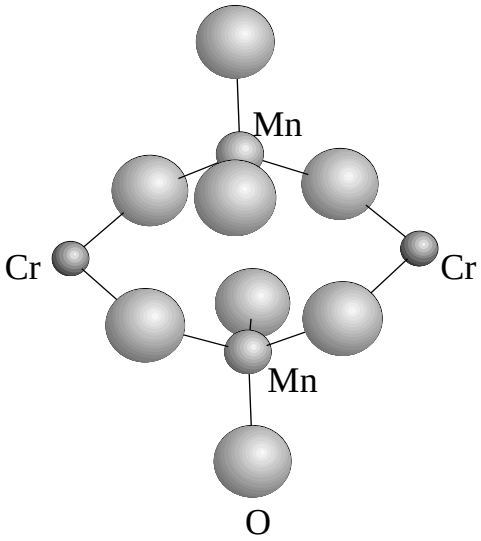

Figure 2. Paths for superexchange interactions.

and $(\frac{1}{4}, \frac{1}{4}, \frac{1}{4})$ respectively, whereas O is at (x, x, x). There are then only two geometrical parameters to optimize: the lattice parameter a and the fractional coordinate of the oxygen atom, x. The nearest-neighbour coordination of Cr, Mn and O is sketched in figure 1 (see page 68 of reference [11] for a figure showing the primitive cell). The Cr and Mn atoms occupy octahedral and tetrahedral sites, respectively. The CrO_6 octahedron is regular only for the ideal geometry ($x = \frac{1}{4}$), whereas the MnO_4 tetrahedron is always regular. It is interesting to notice that each oxygen is fourfold coordinated with one Mn and three Cr nearest neighbours (figure 1). This is also clearly seen in figure 2, which will be used for the discussion of the superexchange interaction. As x increases, the oxygen atoms are displaced along a [111] direction, causing the Mn tetrahedron to expand at the expense of

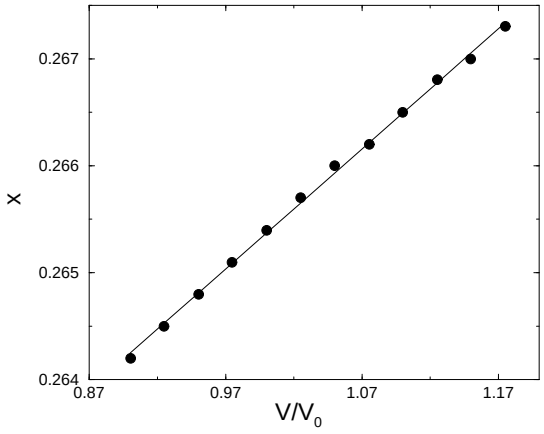

Figure 3. The fractional coordinate, x, as a function of the ratio V/V_0 (V_0 is the experimental cell volume).

Table 1. The lattice parameter, a (Å), oxygen fractional coordinate, x, interatomic distances and angles (degrees) calculated for the equilibrium geometry. Experimental data (see reference [12]) are given for comparison.

	a	x	Mn–O	Cr–O	O–$\widehat{\text{Cr}}$–O	O–$\widehat{\text{Mn}}$–O	Cr–$\widehat{\text{O}}$–Mn	Cr–$\widehat{\text{O}}$–Cr
Experiment	8.437	0.2641	2.03	2.00	83.0 97.0	109.5	120.4	89.7
Calculation	8.582	0.2656	2.09	2.02	82.2 97.8	109.5	119.9	89.6

the Cr octahedron, while the symmetry of the latter ($m3m$ in the ideal case) downgrades to $3m$. However, the Cr–O bond distances remain the same. For the experimental geometry ($a = 8.437$ Å and $x = 0.2641$ [12]), the Cr–O and Mn–O distances are 2.00 and 2.03 Å, respectively; the O–$\widehat{\text{Cr}}$–O angles in the distorted octahedron are 83° and 97°. The calculated equilibrium geometry of $MnCr_2O_4$ for the FEM solution has been obtained from a best fit with respect to the Murnaghan equation of state for 12 volumes ($0.9V_0 < V < 1.175V_0$, V_0 being the experimental volume). At each volume, x has been optimized (see figure 3). The resulting equilibrium lattice parameter is 8.582 Å, with an overestimation with respect to the experimental value of 2%. The calculated fractional coordinate varies linearly with volume and its value at equilibrium ($x = 0.2656$) is in good agreement with experiment. The interatomic distances and angles deduced from the calculated equilibrium geometry are reported in table 1. The angles are very close to the experimental values, as they depend on the x-value only. For the bulk modulus, B, a value of 208.6 GPa has been obtained; we were unable to find an experimental value for comparison. The calculated bulk moduli for Cr_2O_3 and MnO are 262.5 and 164.0 GPa, respectively.

3.2. Electronic behaviour

All of the electronic properties were evaluated for the optimized geometry obtained for the ferromagnetic solution. The results are extremely similar for the ferromagnetic (FEM) and the two ferrimagnetic (FIM_1 and FIM_2) solutions considered here, except the small differences in the spin density that will be discussed below.

The net charges resulting from a Mulliken analysis (see table 2) are +1.85, +2.12 and

Table 2. Mulliken population data (in units of $|e|$): the electron charge ($\alpha + \beta$) and net spin ($\alpha - \beta$) for the atomic orbitals, and the overlap populations (X–O) for ferromagnetic $MnCr_2O_4$. The numbers in parentheses refer to the FIM_1 or FIM_2 solutions, and to oxygen atoms which are first neighbours of a Mn↓ ion.

		Cr		Mn		O	
		$\alpha+\beta$	$\alpha-\beta$	$\alpha+\beta$	$\alpha-\beta$	$\alpha+\beta$	$\alpha-\beta$
Total	sp	18.12	0.03	18.04	0.02	9.52	−0.01 (−0.05)
$d(t_{2g})$		3.10	2.91	3.08	2.93		
$d(e_g)$		0.67	0.12	2.03	1.98		
Total	d	3.77	3.03	5.11	4.91		−0.01 (−0.05)
Grand total		21.89	3.06	23.15	4.93	9.52	
Net charge		+2.12		+1.85		−1.52	
X–O		0.03	−0.01	−0.03	−0.05	−0.02	0.00

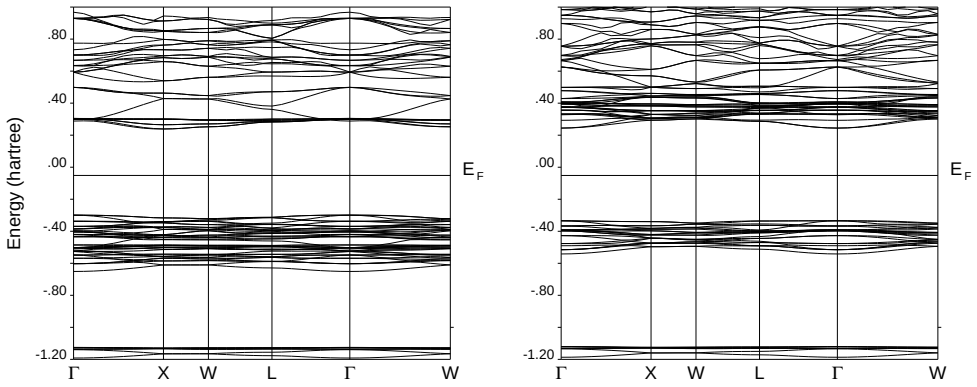

Figure 4. The α (left) and β (right) band structure of ferromagnetic $MnCr_2O_4$. E_F is the Fermi level.

−1.52 $|e|$ for Mn, Cr and O, respectively. By considering the ideal ionic state (Mn^{2+}, Cr^{3+} and O^{2-}) as a reference, the most important modification is the charge transfer of about 0.5 $|e|$ from each nearest-neighbour oxygen atom to Cr, whereas Mn is very close to the ideal situation. Most of the 0.9 $|e|$ transferred to Cr goes to the d shell in e_g states, where both α- and β-states are populated (0.39 and 0.27 $|e|$, respectively). This indicates a certain degree of covalency, which is confirmed by the bond population data: +0.03 $|e|$ for each of the six Cr–O bonds (the same value is observed for Cr_2O_3), whereas the Mn–O bond population is negative (−0.03 $|e|$) indicating a relatively strong repulsion between the two ions.

The band structures of $MnCr_2O_4$ for the α- and β-states of the FEM solution are shown in figure 4; the bands at about −1.2 Hartree are nearly pure oxygen 2s bands; they are separated by a large gap from the upper valence bands, to which the 2p oxygen and the 3d Cr and Mn electrons contribute. In the case of the β band structure, only the 2p oxygen electrons contribute significantly, with minor contributions from Cr d electrons (0.37 $|e|$). The gap between the valence and conduction bands is of 0.55 Hartree, confirming that $MnCr_2O_4$ is quite ionic. The projected density of states (DOS), figure 5, shows that the top

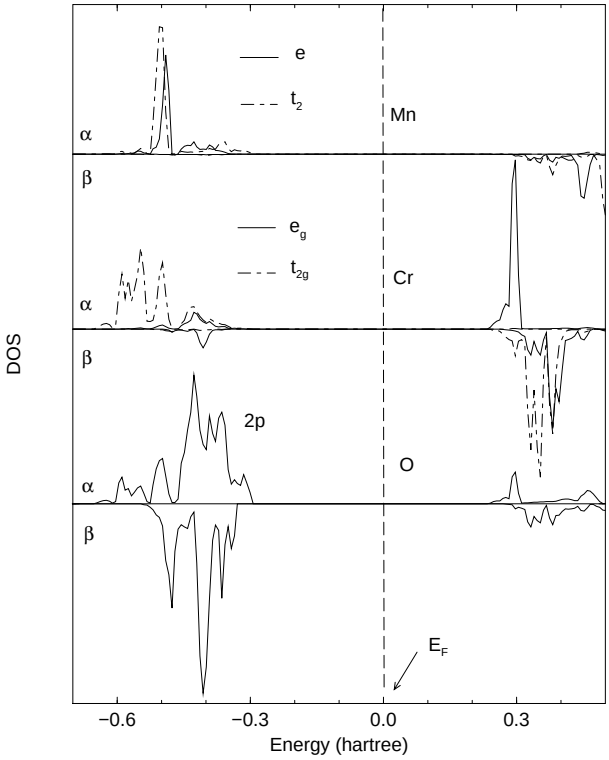

Figure 5. The density of electronic states (DOS) of $MnCr_2O_4$. Projections onto the atomic orbital contributions for the ferromagnetic solution are shown.

of the valence band is mainly contributed by p(O), whereas the bottom of the conduction band is given mainly by d(Cr): so, the energy gap has p–d character, and $MnCr_2O_4$ appears to be an insulator with some charge-transfer character. The Mn d electrons give two sharp peaks at about −0.5 Hartree due to e and t_2 states containing nearly exactly five electrons (table 2), with only minor contributions to the valence bands above and below this value. Almost all of these electrons are in α-states (5.01 $|e|$); the very small contribution from β-states (about 0.1 $|e|$) is due to mixed terms including the contributions of the four nearest-neighbour oxygen atoms. The Cr d states are, in contrast, more diffuse; the large band between −0.6 and −0.45 Hartree is due to t_{2g} α-electrons (3.00 $|e|$). The broad diffuse band between −0.45 and −0.30 Hartree, with contributions from both α and β e_g electrons (0.40 $|e|$ and 0.27 $|e|$ respectively), overlaps with the diffuse oxygen p band, giving rise to a σ-bonding (upper valence bands) σ-antibonding (lower conduction bands) Cr–O interaction. This feature, already observed for Cr_2O_3 (see figure 4 in reference [6]), indicates the presence of some covalent character in the Cr–O bond, as has already been indicated by bond population data.

A map of the electron-density difference between the crystalline charge density and the superposition of the spherical ions Mn^{2+}, Cr^{3+} and O^{2-} (whose wave-function has been obtained with the same basis set as was used for the bulk) is given in figure 6. The usual spherical shrinking of the electron density of the cations and anions in the solid is observed; it is a consequence of the Madelung field and the exchange repulsion. A large redistribution of the Cr charge occurs in the solid, as, due to the crystal field, d levels split and only the

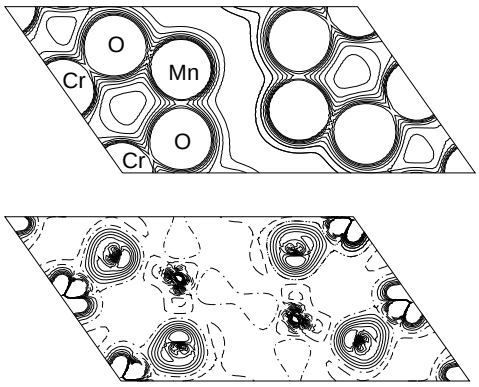

Figure 6. Total and difference (crystal minus ionic superposition) charge-density maps on a plane passing through Mn, O and Cr atoms. The total and difference densities are truncated in the core region at 0.08 and ± 0.03 e/Bohr^{-3}, respectively; the separations between two contiguous isodensity curves are 0.01 and 0.005 e/bohr^{-3}, respectively. Continuous, chain and dashed lines in the difference map indicate positive, zero and negative values, respectively. Notice that, in the difference map, the function is negative in the central lobe of the Cr atom, the one directed towards the oxygen atom, and positive in the two lateral ones.

t_{2g} set is occupied; a deformation of the oxygen charge towards the Cr ions is also observed in the direction of the hole (dashed lines for Cr) created by filling the t_{2g} orbitals. The modification of the charge distribution of Mn is less dramatic than for Cr, because, in the solid, it retains the spherical symmetry of the isolated ion. The features shown by Cr and O in figure 6 are extremely similar to those shown by the same atoms in Cr_2O_3 (see figure 5 in reference [6]).

Table 3. The calculated equilibrium volume, V, and total energy per formula unit, E, for MnO, α-Cr_2O_3 and $MnCr_2O_4$, and the energy difference, ΔE (in kcal mol^{-1}), between $MnCr_2O_4$ and the mixture of oxides. HF + d(O) means that an optimized d shell has been added to the oxygen basis set. HF + P91 + d(O) refers to results including an *a posteriori* evaluation of the correlation energy through Perdew's functional [13].

		MnO	Cr_2O_3	MnO + Cr_2O_3	$MnCr_2O_4$	ΔE
HF	V (Å^3)	23.178	50.249	73.427	79.014	
	E (au)	−1224.8242	−2311.5931	−3536.4173	−3536.4490	19.89
HF + d(O)	V (Å^3)	23.178	50.514	73.692	79.197	
	E (au)	−1224.8251	−2311.6081	−3536.4332	−3536.4666	20.96
HF + P91	V (Å^3)	20.993	46.813	67.806	73.423	
+ d(O)	E (au)	−1226.3126	−2314.7985	−3541.1111	−3541.1382	17.01

3.3. The equilibrium of the spinel decomposition

The calculated equilibrium volumes and energies of MnO, α-Cr_2O_3 and $MnCr_2O_4$ are reported in table 3. At zero pressure and at the static limit, $MnCr_2O_4$ is more stable than the mixture of simple oxides by about 20 kcal mol^{-1} per formula unit at the Hartree–Fock level; basis set improvements, such as the addition of polarization d functions to

oxygen, do not modify this number. As electron correlation effects are expected to play a non-negligible role, they have been estimated *a posteriori* (that is, by using the Hartree–Fock self-consistent charge density) with the correlation-only density functional proposed by Perdew [13]; the recalculated equilibrium volumes and energies are given in table 3. The stability of the spinel with respect to the oxides decreases to 17 kcal mol^{-1}. The $MnCr_2O_4$ experimental enthalpy of formation (see figure 4 of reference [8]) is 15 kcal mol^{-1}. The corrections required for comparing the calculated and the experimental data ($H^{exp} - H^0$ and zero-point vibrational energies) are expected to increase the difference between the two numbers by no more than 2–3 kcal mol^{-1}, so the agreement must be considered very satisfactory. These numbers are similar to those obtained in a previous study with the same method for the equilibrium $MgO + \alpha\text{-}Al_2O_3 \rightleftharpoons MgAl_2O_4$ ($\Delta E = 5.1$ kcal mol^{-1} at the HF-plus-correlation level, to be compared with 5.3 kcal mol^{-1} from experiment). Also, the equilibrium volume differences between the spinel and the mixture of oxides are very similar in the two cases (ΔV is 5.59 and 4.94 $Å^3$ for $MnCr_2O_4$ and $MgAl_2O_4$, respectively). In both cases, the higher stability of the spinel at atmospheric pressure is due to a more efficient exploitation of the electrostatic interactions, only partially compensated by a higher short-range repulsion.

3.4. Ferromagnetic and ferrimagnetic states

In the present study, it was possible to investigate, together with the ferromagnetic solution (FEM, all spins up), two ferrimagnetic solutions, FIM_1 (where one Mn atom has opposite spin with respect to twelve Cr and four Mn second neighbours) and FIM_2 (where all Mn atoms have opposite spin with respect to their own coordination sphere of twelve Cr atoms).

The superexchange paths for the Cr↑–Mn↓ (where the arrows indicate the spin associated to the metal ions) and Mn↑–Mn↓ interactions are shown in figure 2.

Table 4. Total energies per unit cell (in Hartree, for the experimental geometry) at the Hartree–Fock level (E_{HF}) and Hartree–Fock + *a posteriori* correlation-corrected level [13] (E_{HF+P91}). ΔE_{HF} and ΔE_{HF+P91} are the corresponding energy differences with respect to the ferromagnetic (FEM) solution (with all metal spins up). FIM_1 and FIM_2 indicate the two antiferromagnetic solutions (the former contains one Mn↑ (spin up) and one Mn↓ (spin down); the latter contains two Mn↓; in both phases all Cr are ↑).

Solution	E_{HF}	ΔE_{HF}	E_{HF+P91}	ΔE_{HF+P91}
FEM	−7072.882 94	—	−7082.229 35	—
FIM_1	−7072.884 78	0.001 84	−7082.231 52	0.002 17
FIM_2	−7072.886 19	0.003 25	−7082.233 17	0.003 82

Because of computational limitations, we were unable to explore the Cr↑–Cr↓ superexchange interaction; in fact, the point symmetry of a unit cell in which a fraction of Cr atoms possess α-spin and the remaining atoms possess β-spin is very low, and the corresponding computational cost unmanageable at the moment. The total energies of the FEM, FIM_1 and FIM_2 solutions are given in table 4. The energy differences $\Delta E(\text{FEM}-\text{FIM}_1)$ and $\Delta E(\text{FEM}-\text{FIM}_2)$ are measures of the 12Cr↑–Mn↓ + 4Mn↑–Mn↓ and 24Cr↑–Mn↓ interactions, respectively. Under the hypothesis of additivity, it is possible to associate energies of 0.135 (0.159) and 0.054 (0.065) mHartree to each Cr↑–Mn↓ and Mn↑–Mn↓ interaction, respectively, at the HF (HF + P91 [13]) level. It is interesting to notice that the Mn↑–Mn↓ interaction is larger than expected on the basis of the

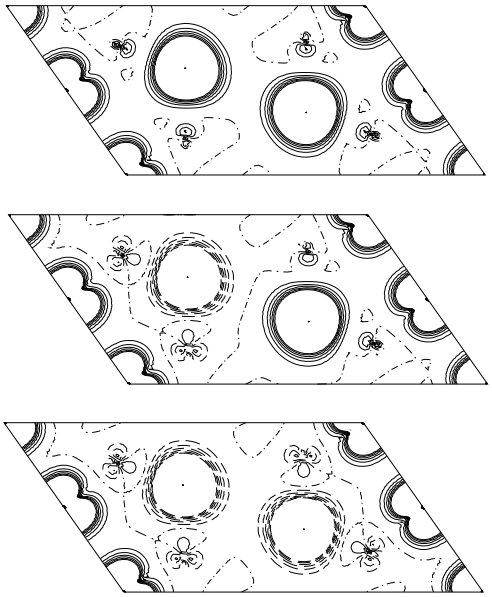

Figure 7. Spin-density maps of the FEM, FIM_1 and FIM_2 phases of $MnCr_2O_4$ in a plane passing through Mn, O and Cr atoms. The plane is the same as in figure 6; the scale corresponds to that used for the difference map. Continuous and dashed lines correspond to an excess of α- and β-electrons, respectively; chain lines correspond to equal values of the two densities.

superexchange path sketched in figure 2: the two atoms interact through a Cr atom and the corresponding bridging oxygen atoms. A direct Mn↑–Mn↓ interaction could be suggested by the relatively short distance (3.7 Å; see figures 6 and 7), but we did not find any trace of it in the population analysis data, or in the spin-density maps (figure 7). As regards the Cr↑–Mn↓ interaction, the usual interpretation scheme can be adopted, as in reference [14]: in the FEM state, the oxygen ion is surrounded by four metal ions whose external electrons have α-spin; the short-range Cr–O and Mn–O repulsion then involves mainly the oxygen α-electrons; as a consequence, there is a small spin polarization on the oxygen (see figure 7 and table 2). In the FIM_2 state, the oxygen ions are surrounded by ions with α (three Cr) and β (one Mn) d electrons; small displacements of the α- or β-electrons on oxygen towards ions with opposite spin are sufficient to reduce the 'spin pressure' of the FEM solution. The total amount of charge involved in this movement is very small (less than 0.1 $|e|$; see table 2); one should remember, however, that the energy differences are very small too (about 4 mHartree; see table 4). The FIM_1 situation is intermediate between the FEM and FIM_2 cases. The spin polarization on the anion, and the mechanism connected to the stabilization of antiferromagnetic alignments are less evident here (see figure 7) than in other cases, where the anion is twofold coordinated with an M–$\widehat{\text{O}}$–M angle of 180° [14]; the threefold-coordinated anion, as in rutile-type MnF_2 structures [5, 6], is intermediate between the two previous types.

According to some authors, the spin ordering in $MnCr_2O_4$ is not of the ferrimagnetic collinear type discussed here, but involves more complicated spin orientations (spiral ordering; see figure 18 in reference [11]). However, limitations in both the Hamiltonian adopted (the UHF method provides spin-polarized states that are eigenfunctions of the spin operator S_z, but not of S^2) and the computational resources (some ferrimagnetic structures

would require magnetic cells much larger than the non-magnetic one, with a substantial reduction of the point symmetry and subsequent increase in computational cost) prevent the exploration of these possibilities in the present work.

4. Conclusions

An *ab initio* quantum mechanical treatment has been successfully applied to the study of a relatively complicated crystalline structure, containing 14 atoms/cell, including six transition metal atoms (four Cr and two Mn). The solid-state chemical reaction $MnO + \alpha Cr_2O_3 \rightleftharpoons MnCr_2O_4$ has been investigated; the results compare well with experiment and are of the same quality as those obtained for similar reactions between systems containing lighter atoms [11]. The electronic structure has been shown to be very close to the ideal ionic one for Mn (net charge $+1.85\ |e|$, 5.11 unpaired d electrons), whereas a relatively large O $\rightarrow$ Cr back-donation takes place with respect to the O^{2-}, Cr^{3+} formal charges. Two ferrimagnetic states have been considered, which are more stable than the ferromagnetic one. The Mn↑–Mn↓ superexchange interaction turns out to be far from negligible, although, as expected, it is smaller than the Cr↑–Mn↓ one.

Acknowledgments

This work was supported by the Human Capital and Mobility Programme of the European Union under contract CHRX-CT93-0155, and by the the Italian MURST (40%) and Italian CNR.

References

[1] Pisani C, Dovesi R and Roetti C 1988 *Hartree–Fock ab initio Treatment of Crystalline Systems (Springer Lecture Notes in Chemistry 48)* (Heidelberg: Springer)
[2] Saunders V R, Freyria-Fava C, Dovesi R, Salasco L and Roetti C 1992 *Mol. Phys.* **77** 629
[3] Mackrodt W C, Harrison N M, Saunders V R, Allan N L, Towler M D, Aprà E and Dovesi R 1993 *Phil. Mag.* **68** 653
[4] Towler M D, Allan N L, Harrison N M, Saunders V R, Mackrodt W C and Aprà E 1994 *Phys. Rev.* B **50** 5041
[5] Catti M, Valerio G and Dovesi R 1995 *Phys. Rev.* B **51** 7441
[6] Catti M, Sandrone G, Valerio G and Dovesi R 1996 *J. Phys. Chem. Solids* **57** 1735
[7] Dovesi R, Saunders V R, Roetti C, Causà M, Harrison N M, Orlando R and Aprà E 1996 *CRYSTAL95 User's Manual* (Torino: University of Torino)
[8] Krupička S and Novák P 1982 *Ferromagnetic Materials* vol 3, ed E P Wohlfarth (Amsterdam: North-Holland) ch 4
[9] Catti M, Valerio G, Dovesi R and Causà M 1994 *Phys. Rev.* B **49** 14 179
[10] Aprà E 1993 *PhD Thesis* University of Torino
[11] Adams D M 1974 *Inorganic Solids. An Introduction to Concepts in Solid-State Structural Chemistry* (London: Wiley)
[12] Raccah P M, Bouchard R J and Wold A 1966 *J. Appl. Phys.* **37** 1436
[13] Perdew J P 1986 *Phys. Rev.* B **33** 8822 (errata 1986 **34** 7406)
Perdew J P, Chevary J A, Vosko S H, Jackson K A, Pederson M R, Singh D J and Fiolhais C 1992 *Phys. Rev.* B **46** 6671
[14] Ricart J M, Dovesi R, Roetti C and Saunders V R 1995 *Phys. Rev.* B **52** 2381 (errata 1997 **55** 15 942)